

## Preparation of $\text{Lu}_2\text{O}_3:\text{Eu}^{3+}$ nanopowders for optical ceramics

*R.P.Yavetskiy*

Institute for Single Crystals, STC "Institute for Single Crystals", National Academy of Sciences of Ukraine, 60 Lenin Ave., 61001 Kharkiv, Ukraine

*Received September 5, 2008*

The  $\text{Lu}_2\text{O}_3:\text{Eu}^{3+}$  (1 at. %) nanopowders have been obtained by precipitation from aqueous solution using ammonium hydrocarbonate as the precipitant. The influence of the calcination temperature on the morphology, average particle size and sinterability of  $\text{Lu}_2\text{O}_3:\text{Eu}^{3+}$  powders have been studied. It has been shown that the calcination temperature of  $1000^\circ\text{C}$  provides the preparation of low-agglomerated fine powders of europium doped lutetium oxide with spherical particles and high surface activity that can be used as a starting material for transparent ceramics manufacturing.

Методом осаждения из водных растворов с использованием гидрокарбоната аммония в качестве осадителя получены нанопорошки  $\text{Lu}_2\text{O}_3:\text{Eu}^{3+}$  (1 ат. %). Изучено влияние температуры прокаливания на морфологию, средний размер частиц и спекаемость порошков  $\text{Lu}_2\text{O}_3:\text{Eu}^{3+}$ . Показано, что температура прокаливания  $1000^\circ\text{C}$  позволяет получить активные низкоагломерированные дисперсные порошки  $\text{Lu}_2\text{O}_3:\text{Eu}^{3+}$  с частицами сферической формы, которые могут быть использованы в качестве исходного материала для получения прозрачной керамики.

Lutetium oxide  $\text{Lu}_2\text{O}_3$  is a material of good promises for various spectroscopic applications due to its high chemical stability, transparency in a wide wavelength range and high isomorphous capacity for doping with luminescent rare-earth ions. For example, excellent thermal and mechanical properties make it possible to consider  $\text{Lu}_2\text{O}_3$  as a promising matrix for high-power solid state lasers, laser fusion drivers, etc. [1].  $\text{Lu}_2\text{O}_3:\text{Eu}^{3+}$  is a prospective scintillator for medical imaging, for instance, for X-ray computer-aided tomography [2, 3].  $\text{Lu}_2\text{O}_3:\text{Yb}^{3+}$  has been studied as a scintillation material possessing charge transfer luminescence in trivalent ytterbium ions [4], and  $\text{Lu}_2\text{O}_3:\text{Tb}$ , as an effective storage phosphor [5]. However, the manufacture of  $\text{Lu}_2\text{O}_3$  single crystals meets significant difficulties due to extremely high melting point of the compound ( $2490^\circ\text{C}$ ). There is only few works aimed at production of  $\text{Lu}_2\text{O}_3$  single crystals, but no crystals of

necessary size and optical quality were obtained.

Recent advances in optical ceramic production make it possible to obtain a polycrystalline bulk material, which has structural, functional and economical advantages over the corresponding single crystals. So, the ceramics enables higher dopant concentrations with controlled distribution over the ceramic body volume, reproducible optical spectra; its production requires reduced general cost compared to single crystal pulling by conventional methods. These advantages are based on utilization of nanotechnology and pressure-free vacuum sintering method [6]. To produce transparent ceramics, the fine non-agglomerated nanopowders with average spherical particle size of about 100 nm are required. Nowadays, various wet chemical processes were used to produce  $\text{Lu}_2\text{O}_3:\text{Eu}^{3+}$  nanopowders, including the combustion synthesis [7], molten salt technique [8], and co-precipitation method. However,

utilization of conventional chemical precipitation techniques allows one to provide nanosized powders with characteristics required to produce optical ceramics. Just recently the light yield of 90000 photons/MeV was achieved with  $\text{Lu}_2\text{O}_3:\text{Eu}^{3+}$  (5 at. %) ceramics consolidated from co-precipitated nanopowders. Therefore, the purpose of this work is to obtain  $\text{Lu}_2\text{O}_3:\text{Eu}^{3+}$  well-sinterable nanopowders for optical ceramics using conventional co-precipitation.

$\text{Lu}_2\text{O}_3:\text{Eu}^{3+}$  (1 at. %) nanopowders were obtained by co-precipitation technique using ammonium hydrocarbonate  $\text{NH}_4\text{HCO}_3$  (>99.5 % purity) as the precipitant. The relatively low europium concentration (1 at. %) was chosen to exclude possible influence of the activator on sintering of  $\text{Lu}_2\text{O}_3:\text{Eu}^{3+}$  powders. Aqueous lutetium and europium nitrate solution was prepared by dissolving the corresponding oxides (99.99 % purity) in nitric acid. The precursor precipitate was produced by adding a mother solution to ammonium hydrocarbonate (reverse strike method) under mild stirring at room temperature. The resultant suspension was aged for 24 h, filtered using suction, washed thoroughly several times by deionized water and ethyl alcohol, and finally dried at  $120^\circ\text{C}$  for 24 h. Then, the precursor was calcined at 550, 700, 1000 and  $1200^\circ\text{C}$  for 2 h to obtain europium doped lutetium oxide.

The IR absorption spectra were obtained using a Spectrum One FT-IR spectrometer (Perkin Elmer) with KBr pellets. Differential thermal (DTA) and thermogravimetric (TG) analysis of the precursor was carried out using a MOM Q-1500D derivatograph (Hungary) at the heating rate of  $5^\circ\text{C}/\text{min}$  and  $\alpha\text{-Al}_2\text{O}_3$  as a reference. The phase characterization of the precursor and calcined powders was performed by the X-ray diffraction (XRD) method using a DRON-4 diffractometer (Russia) in  $\text{FeK}_\alpha$  radiation in the  $2\theta$  range of 20 to 80 degrees. The specific surface area was measured using BET method with home-made setup. The powder morphology was observed by transmission electron microscopy (TEM-125, Russia) and by scanning electron microscopy (JSM-6390 LV, JEOL, Japan). The sintering of nanopowders was studied using a NETZSCH 402 ED dilatometer in the 20 to  $1480^\circ\text{C}$  temperature range in constant rate heating mode.

The IR spectra of precursor dried at  $50^\circ\text{C}$  and of  $\text{Lu}_2\text{O}_3$  powders calcined at 800 and  $1200^\circ\text{C}$  for 2 h are presented in Fig. 1. The broad absorption band at  $3435\text{ cm}^{-1}$  was at-

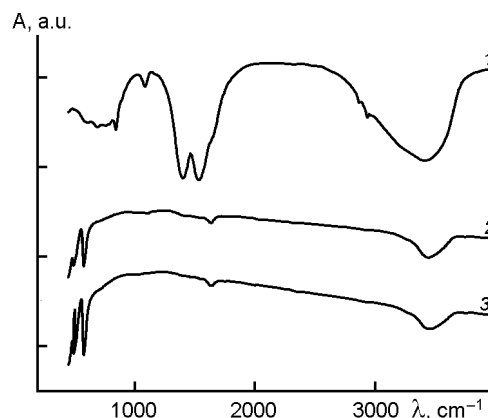


Fig. 1. FT-IR spectra of the precipitated precursor (1) and  $\text{Lu}_2\text{O}_3:\text{Eu}^{3+}$  (1 at. %) powders, calcined at  $800^\circ\text{C}$  (2) and  $1200^\circ\text{C}$  (3).

tributed to O-H stretching. The wide absorption bands at  $1525\text{--}1530$  and  $1385\text{--}1400\text{ cm}^{-1}$  were assigned to C-O asymmetric stretch in  $\text{CO}_3^{2-}$ . The absorption peaks at  $1075\text{--}1085\text{ cm}^{-1}$  and  $840\text{--}850\text{ cm}^{-1}$  appearing in the precursor sample are probably connected with stretching and bending of C-O band [9]. These peaks may evidence the presence of carbonate groups in the precursor. The precursor calcination at  $800\text{--}1200^\circ\text{C}$  results in lutetium oxide formation. The absorption peaks at  $498$  and  $580\text{ cm}^{-1}$  in the spectra of sample calcined at  $800^\circ\text{C}$  are characteristic peaks related to Lu-O stretching [10], indicating the crystallization of lutetium oxide. Several residual weak absorption bands were attributed to  $\text{H}_2\text{O}$  and  $\text{CO}_2$  absorbed at the powder surface in air atmosphere. Their absorption intensity decreases with increasing calcination temperature.

The DTA-TG traces of precursor after its drying at room temperature are illustrated in Fig. 2. A continuous sample mass loss is observed up to  $650^\circ\text{C}$  and amounts 32 %. Endothermic peaks in the DTA curve at  $130^\circ\text{C}$  and in the  $200\text{--}600^\circ\text{C}$  temperature range correspond to release of molecular and hydration water, and to decomposition of precursor (which is probably lutetium carbonate). The lutetium oxide formation occurs at a relatively low temperature and is over at  $650^\circ\text{C}$ . Recently it has been shown [7] that the lutetium nitrate precipitation with mixed precipitant ( $\text{NH}_4\text{HCO}_3 + \text{NH}_3\cdot\text{H}_2\text{O}$ ) results in the formation of basic lutetium carbonate. The precursor composition has not been studied in this work; however, FT-IR spectra and DTA-TG curves of precipitated precursor are in a good agree-

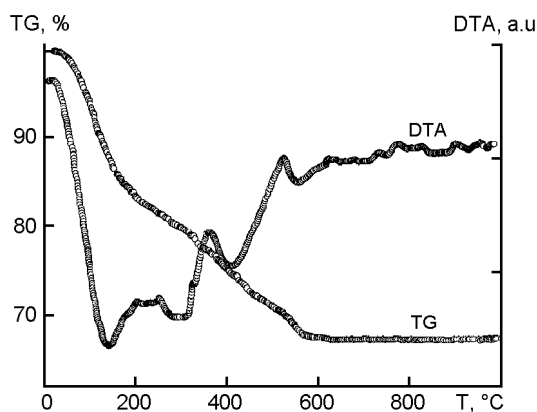


Fig. 2. DTA-TG curves of the precursor prepared using  $\text{NH}_4\text{HCO}_3$ .

ment with the data [7]. For this reason, we suppose that the precursor composition is  $\text{Lu}(\text{OH})_x(\text{CO}_3)_y \cdot n\text{H}_2\text{O}$ .

The XRD analysis of  $\text{Lu}_2\text{O}_3:\text{Eu}^{3+}$  powders calcined at various temperatures for 2 h are presented in Fig. 3. According to the XRD data, the precursor and products of its calcination at  $T < 550^\circ\text{C}$  are amorphous. The formation of cubic lutetium oxide starts at  $550^\circ\text{C}$ . The temperature increase from 550 to  $1000^\circ\text{C}$  causes the half-width decrease of diffraction peaks and their intensity increase. This indicates an improvement of  $\text{Lu}_2\text{O}_3:\text{Eu}^{3+}$  crystallinity. The average crystallite size estimated by Scherrer equation also increases from 10.5 to 30.5 (Fig. 4, 3). All the diffraction peaks in the XRD patterns were attributed to cubic  $\text{Lu}_2\text{O}_3:\text{Eu}^{3+}$ .

The specific surface area values  $S_{\text{BET}}$  and crystallite size of obtained powders calculated from Scherrer equation ( $d_{\text{XRD}}$ ) and estimated from specific surface area ( $d_{\text{BET}}$ ), considerably depends on the calcination temperature, Fig. 4. The precursor dried at  $120^\circ\text{C}$  is characterized by high specific surface area  $S_{\text{BET}} = 45\text{--}50 \text{ m}^2/\text{g}$  (not shown in Fig. 4). The temperature increase from 550 to  $1200^\circ\text{C}$  results in decreasing  $S_{\text{BET}}$  value of  $\text{Lu}_2\text{O}_3:\text{Eu}^{3+}$  nanopowders from 17 to  $4 \text{ m}^2/\text{g}$ . This is accompanied by simultaneous increase of crystalline size  $d_{\text{BET}}$  from 30 to 175 nm. TEM images were used to characterize and compare the microstructure of nanopowders calcined at various temperatures (Fig. 5). The powders calcined at  $T < 700^\circ\text{C}$  possess a high agglomeration extent due to low primary crystalline size. Increase of the crystallite size results in decrease of the agglomeration extent due to strong reduction of particle interaction forces (Fig. 5, a). At the optimum calcina-

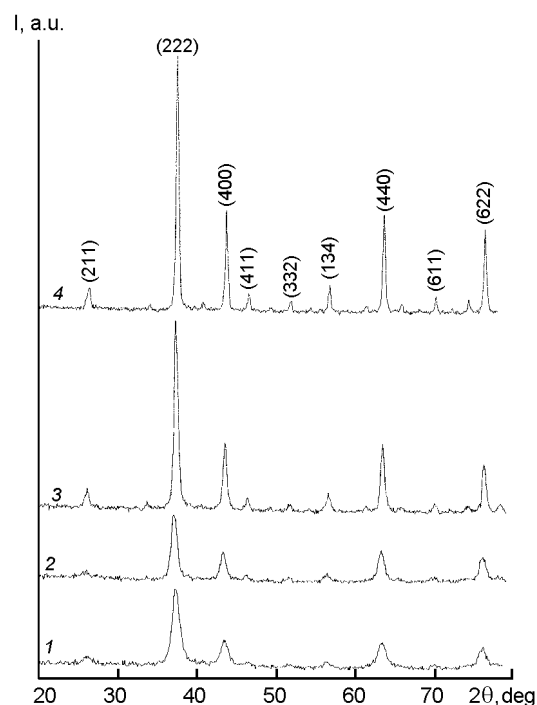


Fig. 3. XRD patterns of  $\text{Lu}_2\text{O}_3:\text{Eu}^{3+}$  powders calcined at  $T$  ( $^\circ\text{C}$ ): 550 (1); 600 (2); 800 (3), 1200 (4).

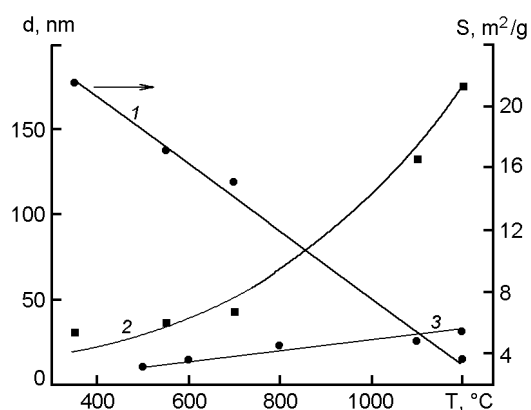


Fig. 4. Dependences of specific surface area  $S_{\text{BET}}$  (1) and average crystalline size obtained using BET method,  $d_{\text{BET}}$  (2) and XRD data,  $d_{\text{XRD}}$  (3) vs. precursor calcination temperature.

tion conditions ( $T = 1000^\circ\text{C}$ ), all the particles of  $\text{Lu}_2\text{O}_3:\text{Eu}^{3+}$  powders have nearly spherical form, the average particle size being 25–30 nm and  $S_{\text{BET}}$ ,  $8 \text{ m}^2/\text{g}$ . The particles are only slightly agglomerated, and agglomerates have spherical shape (Fig. 5, b). These powders possess favorable morphology features (particle size and shape, agglomeration extent, surface activity) to be used as a starting material for transparent ceramics production. The average particle size determined from TEM data

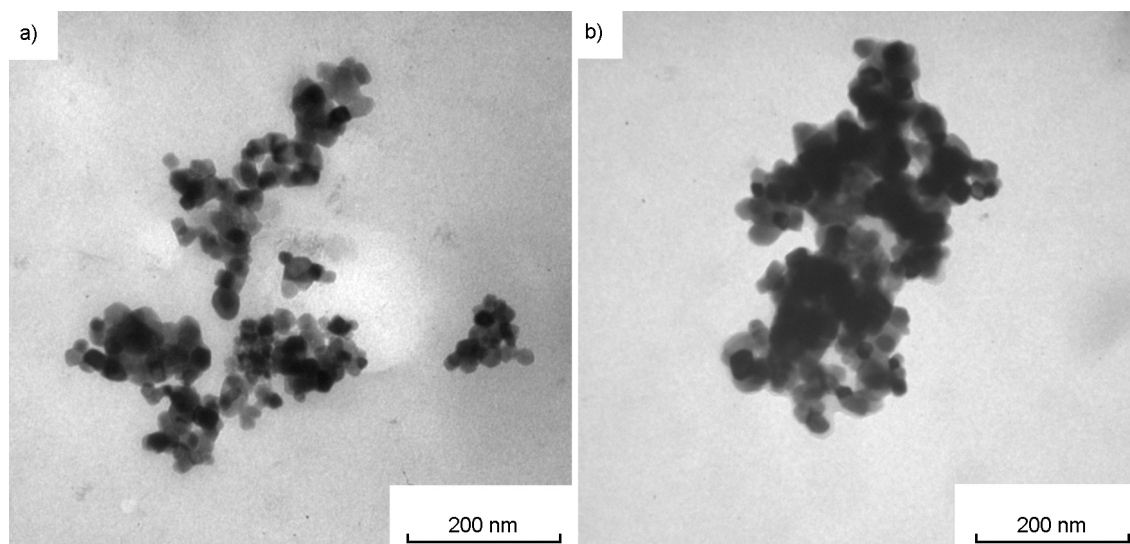


Fig. 5. TEM of  $\text{Lu}_2\text{O}_3:\text{Eu}^{3+}$  powders calcined at  $700^\circ\text{C}$  (a) and  $1000^\circ\text{C}$  (b) for 2 h.

has been found to be in a good agreement with the corresponding values calculated using the Scherrer equation, while significantly differing from the particle size estimated from specific surface area. Perhaps this difference is due to the fact that, when using the specific surface area value  $S_{BET}$ , we do not obtain the primary particle size, but the size of agglomerates (Fig. 4).

The sinterability of  $\text{Lu}_2\text{O}_3:\text{Eu}^{3+}$  nanopowders calcined at various temperatures was studied using the sintering method at constant heating rate. The  $\text{Lu}_2\text{O}_3:\text{Eu}^{3+}$  powders were compacted by conventional uniaxial pressure in one batch under 330 MPa pressure. The green bodies compacted from  $\text{Lu}_2\text{O}_3:\text{Eu}^{3+}$  nanopowders calcined at 550, 700, 1000 and  $1200^\circ\text{C}$  have the relative density of 30, 38, 43 and 49 % (Fig. 6). The calcination temperature increase results in higher densification onset temperature due to particle size growth and decrease of the surface activity (Fig. 6). The  $\text{Lu}_2\text{O}_3:\text{Eu}^{3+}$  powders calcined at 550, 700, 1000 and  $1200^\circ\text{C}$  densify to the relative densities of 75, 58, 84 and 70 %. According to Fig. 6, the best sinterability is shown by  $\text{Lu}_2\text{O}_3:\text{Eu}^{3+}$  powders calcined at  $1000^\circ\text{C}$ , being densified up to 84 % of theoretical value. The presence of hard agglomerates in the powders hinders considerably the compaction and results in a poor sinterability. For example, the powders calcined at  $550^\circ\text{C}$  have the highest  $S_{BET}$  value and, respectively, the highest activity, however, are strongly agglomerated due to low crystallite size. The severe agglomeration hinders the formation of homogenous green compact,

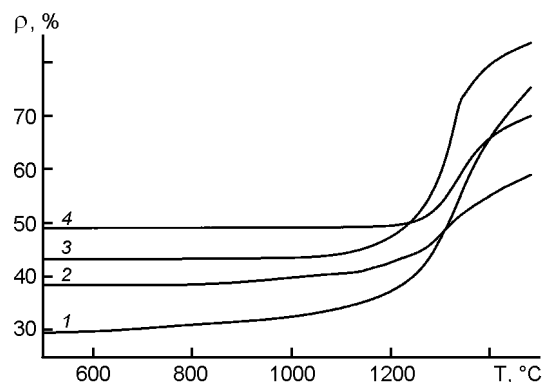


Fig. 6. Relative density vs. temperature for  $\text{Lu}_2\text{O}_3:\text{Eu}^{3+}$  (1 at. %) powders calcined at  $T$  ( $^\circ\text{C}$ ): 550 (1); 700 (2); 1000 (3), 1200 (4).

and hence limits the powders density, to a lower extent ( $\rho = 75\%$ ). On the other hand, the still high shrinkage extent of the powders calcined at  $550^\circ\text{C}$  causes in some cases the cracking of compact after heating. The powders obtained at  $1200^\circ\text{C}$ , despite the highest green density, are poorly sintered (up to 70 % of theoretical value) due to increased particle size and, respectively, a drastically decreased surface activity. Thus, the optimal calcination temperature for reactive  $\text{Lu}_2\text{O}_3:\text{Eu}^{3+}$  nanopowders is  $1000^\circ\text{C}$ . We suppose that using these powders, we will manage to achieve the high final density and to obtain transparent  $\text{Lu}_2\text{O}_3:\text{Eu}^{3+}$  scintillation ceramics by vacuum sintering, which is the subject of our further studies.

To conclude, the  $\text{Lu}_2\text{O}_3:\text{Eu}^{3+}$  (1 at. %) nanopowders have been prepared by co-precipitation using ammonium hydrocarbonate

as the precipitant. Basing on FT-IR spectra and DTA-TG data, the precursor composition has been supposed to be  $\text{Lu}(\text{OH})_x(\text{CO}_3)_y \cdot n\text{H}_2\text{O}$ . It has been shown that the precursor calcination at 550°C and higher results in formation of crystalline lutetium oxide. It has been found that a reactive  $\text{Lu}_2\text{O}_3:\text{Eu}^{3+}$  low-agglomerated spherical particles with specific surface area of 8 m<sup>2</sup>/g and average particle size of 25–30 nm can be obtained by the precursor calcination at 1000°C. These powders possess favorable features (particle size and shape, agglomeration extent, surface activity) to be used as a starting material for  $\text{Lu}_2\text{O}_3:\text{Eu}^{3+}$  transparent ceramics production.

The author is grateful to Dr. T.I.Korshikova and Dr. E.A.Vovk for their assistance in experimental work.

### References

1. J.Lu, K.Takaichi, T.Uematsu et al., *Appl. Phys. Lett.*, **81**, 4324 (2002).
2. A.Lempicki, C.Brecher, P.Szupryczynski et al., *Nucl. Instrum. Meth. Phys. Res. A*, **488**, 579 (2002).
3. Q.Chen, Y.Shi, L.An et al., *J. Am. Ceram. Soc.*, **89**, 2038 (2006).
4. N.V.Guerasimova, I.A.Kamenskikh, D.N.Krasikov et al., in: Proc. of 8<sup>th</sup> Int. Confer. on Inorganic Scintillators and their Use in Scientific and Industrial Applications, ed. by A.Gektin, B.Grinyov, NTS "Institute for Single Crystals", Kharkiv (2006), p.47.
5. E.Zych, J.Trojan-Piegza, D.Hreniak, W.Strek, *J. Appl. Phys.*, **94**, 1318 (2003).
6. Jap. Patent 10-101333 (1998); Jap. Patent 10-101411 (1998).
7. E.Zych, D.Hreniak, W.Strek, *J. Alloys and Compounds*, **341**, 385 (2002).
8. J.Trojan-Piegza, E.Zych, *J. Alloys and Compounds*, **380**, 118 (2004).
9. Q.Chen, Y.Shi, L.An et al., *J. Europ. Ceram. Soc.*, **27**, 191 (2007).
10. N.T.McDevitt, W.L.Baun, *Spectrochim. Acta*, **20**, 799 (1964).

## Одержання нанопорошків $\text{Lu}_2\text{O}_3:\text{Eu}^{3+}$ для виготовлення оптичної кераміки

*Р.П.Явецький*

Методом осадження з водних розчинів з використанням гідрокарбонату амонію як осаджувача одержано нанопорошки  $\text{Lu}_2\text{O}_3:\text{Eu}^{3+}$  (1 ат. %). Вивчено вплив температури прожарювання на морфологію, середній розмір частинок та здатність до спікання порошків  $\text{Lu}_2\text{O}_3:\text{Eu}^{3+}$ . Показано, що температура прожарювання 1000°C дозволяє отримати низькоагломеровні дисперсні порошки  $\text{Lu}_2\text{O}_3:\text{Eu}^{3+}$  з частинками сферичної форми, які мають високу активність та можуть бути використані як вихідний матеріал для отримання прозорої кераміки.